Fused Organic Salts. IV.[1a] Characterization of Low-Melting Quaternary Ammonium Salts. Phase Equilibria for Salt–Salt and Salt–Nonelectrolyte Systems. Properties of the Liquid Salt Medium

John E. Gordon[1b]

Contribution from the Mellon Institute, Pittsburgh, Pennsylvania 15213.
Received March 1, 1965

A set of 20 quaternary ammonium salts ($R_4N^+X^-$, R = n-butyl to n-heptyl), half of them new compounds, which possess especially low melting points was prepared and characterized. The following anions are represented by salts with m.p. $\leq 100°$: I^-, Br^-, SCN^-, ClO_4^-, NO_3^-, and picrate. Solid–liquid phase diagrams for 30 binary salt–salt systems within this set, and for 50 systems of the salts with various nonelectrolytes, were studied in various degrees of detail by hot-stage microscopy. Continuous solid solubility predominates in the salt–salt systems with a common cation, the major exceptions being the picrate-containing systems. Continuous series of solid solutions were observed in the cation-variable systems only when the difference in cation structure amounted to only one methylene group. Fifteen new molecular compounds observed in the salt–nonelectrolyte diagrams, principally of the type R_4N^+-$(AH)_n\cdots X^-$ formed from hydrogen-bridging proton donors, are described. The mutual liquid–liquid solubility behavior for 66 salt–nonelectrolyte systems was qualitatively studied, critical solution temperatures being measured when these fell in the accessible liquid range, ca. (f.p. $-10°$) to 200°. These molten salts are completely miscible near their freezing points with most organic nonelectrolytes, excluding only nonaromatic hydrocarbons and highly associated polar liquids. The incomplete miscibility with highly polar liquids arises from the poorly cohesive nature of these molten $R_4N^+X^-$, three approximate experimental measures agreeing in assigning their cohesive energy densities in the vicinity of that of acetone. Measurements of the spectra of some electron acceptor–X^- charge-transfer complexes in molten $R_4N^+X^-$ indicate enhanced donor reactivity of X^- in this medium.

There are at least four sources of interest in molten organic salts. (1) Their low freezing points bring a fused-salt chemistry of sorts into the temperature range of standard equipment and instrumentation. (2) They provide a new tool for physical organic chemical investigation, *e.g.*, of less stable organic complex ions *via* spectroscopy, cryoscopy, ionography, etc. (3) They are capable of subtle and nearly continuous structure variation. (4) They show promise as interesting reagents and media for organic reactions.[1c] However, despite the experimental difficulties of inorganic fused-salt study, much more is known about inorganic than about organic fused salts.[2] The greatest deterrents to study of the latter are probably (1) lack of information on which salts are both especially low melting and readily obtained in pure condition, (2) a reputation for instability, and (3) lack of data of the most fundamental kind on solubility of nonelectrolytes and inorganic salts in the melts and on the relevant solid–liquid phase diagrams for salt–salt and salt–nonelectrolyte systems. The present study was undertaken to obtain basic information on some of these points and thus provide the necessary foundation for further experiments with these materials.

In the first instance, tetra-*n*-alkylammonium salts have been selected for study. This choice follows from the desirability of a variable organic cation dictated by interest in the study of donor properties of nucleophilic anions in the melts, from their relatively greater availability, and from the absence of light-absorbing structural features which would prohibit electronic spectroscopy in the molten salt medium. Consideration has been limited to quaternary salts since for many uses the presence of acidic NH^+ protons is undesirable. Investigation of the chemical stability of these melts is being reported separately.[1a]

Experimental Section

General. Salts (which, if not prepared as described below (see Table I), were commercially available) were crystallized three or more times and were dried at room temperature and *ca.* 10^{-4} mm. The solid nonelectrolytes employed for calibration of the hot stages and many of those used in the phase diagram studies were highly purified, sublimed materials. Liquid nonelectrolytes used in the critical solution temperature (c.s.t.) measurements were high quality commercial samples but were not further purified. Infrared spectra were recorded on a Beckman IR-9 instrument. N.m.r. spectra were measured with a Varian A-60 spectrometer. X-Ray powder patterns were measured with a Phillips diffractometer. Combustion analyses were performed by Galbraith Laboratories, Inc. Boiling points are uncorrected.

Preparation of Salts. The following preparations illustrate the procedures used. Details for all of the salts are given in Table I.

(1) (a) Part III: J. E. Gordon, *J. Org. Chem.*, 30, 2760 (1965); (b) Woods Hole Oceanographic Institution, Woods Hole, Mass, 02543; (c) J. E. Gordon, *J. Am. Chem. Soc.*, 87, 1499 (1965); (d) *ibid.*, 86, 4492 (1964).

(2) A summary of the literature is given in ref. 1b, to which the following may be added: (a) R. P. Seward, *Inorg. Chem.*, 3, 1056 (1964) (system: Bu_4NClO_4–C_6H_6); (b) T. J. Plati and E. G. Taylor, *J. Phys. Chem.*, 68, 3426 (1964) (system: Bu_4NNO_3–C_6H_6); (c) A. Kisza, *Bull. Acad. Polon. Sci. Ser. Sci. Chim.*, 12, 707, 713 (1964) (e.m.f. measurements in molten dimethylammonium chloride); (d) G. P. Smith, C. H. Liu, and T. R. Griffiths, *J. Am. Chem. Soc.*, 86, 4796 (1964) (inorganic complex ion spectra in fused 'onium salts); (e) H. K. Hofmeister and J. R. Van Wazer, *J. Phys. Chem.*, 69, 791 (1965) (CH_3 exchange in the system ammonium chloride–tetramethylammonium chloride).

Table I. Preparation and Characterization of Tetra-*n*-alkylammonium Salts

Salt	Formula	X, % Calcd.	X, % Found	X	Crystn. solvent	Method of prepn.	Yield, %
Pe_4NBr	$C_{20}H_{44}NBr$	21.11	21.09[a] 21.09[a]	Br	CCl_4–Et_2O, C_6H_6–Et_2O	A	78
Pe_4NI	$C_{20}H_{44}NI$	29.83	29.64[a] 29.73[a] 29.69[a]	I	EtOAc–EtOH	*b*	
$Pe_4N\ NO_3$	$C_{20}H_{44}N_2O_3$	17.20	17.10[c]	NO_3	EtOAc, EtOAc–Et_2O	C	95
$Pe_4N\ NO_2$	$C_{20}H_{44}N_2O_2$	8.13	8.05[d]	N	EtOAc–Et_2O	*e*	83
Pe_4NClO_4	$C_{20}H_{44}NClO_4$	24.99	25.03[c]	ClO_4	EtOH–H_2O	D	89
Pe_4NSCN[f]	$C_{21}H_{44}N_2S$	16.28	16.28[a]	SCN	EtOAc	F	74
Pe_4NPic	$C_{26}H_{46}N_4O_7$	43.31	43.32[g]	Pic	EtOH–Et_2O	E	55
Hex_4NI	$C_{24}H_{52}NI$	26.35	26.52[d]	I	EtOAc	*b*	
Hex_4NClO_4	$C_{24}H_{52}NClO_4$	3.08	3.10[d]	N	EtOH–H_2O, EtOAc–Et_2O	D	97
Hex_4NBr[f]	$C_{24}H_{52}NBr$	18.39	18.45[d]	Br	EtOAc–Et_2O	*b*	
$Hex_4N\ NO_3$	$C_{24}H_{52}N_2O_3$	6.72	6.75[d]	N	EtOAc–Et_2O	C	91
$Hex_3HeptNI$	$C_{25}H_{54}NI$	25.61	25.38[d]	I	EtOAc–Et_2O	A	88
$Hex_3HeptNBr$	$C_{25}H_{54}NBr$	17.81	17.71[d]	Br	EtOAc–Et_2O	G	49
$Hex_3HeptNClO_4$	$C_{25}H_{54}NClO_4$	2.99	2.85[d]	N	EtOAc–Et_2O, H_2O–EtOH	D	85
$Hex_3HeptN\ NO_3$	$C_{25}H_{54}N_2O_3$	6.50	6.52[d]	N	EtOAC–Et_2O	C	94
Hex_2Hept_2NI	$C_{26}H_{56}NI$	24.90	24.67[d]	I	EtOAc–Et_2O	B	57
$Hex_2Hept_2NClO_4$	$C_{26}H_{56}NClO_4$	2.90	2.99[d]	N	EtOH–H_2O	D	82
$Hept_4NI$	$C_{28}H_{60}NI$	23.60	23.47[d]	I	C_6H_6–isooctane	*b*	
$Hept_4NClO_4$	$C_{28}H_{60}NClO_4$	2.75	2.93[d]	N	EtOH–H_2O	D	88
$Hept_4NBr$	$C_{28}H_{60}NBr$	16.29	16.46[d]	Br	EtOAc–Et_2O	*b*	

[a] By Volhard titration of a 0.5-mmole sample in 50% aqueous methanol. [b] Commercially available (Distillation Products Industries). [c] A 0.5-mmole sample in 50–75% aqueous methanol was passed through a column of 10 ml. of Dowex 1–X4, 50–100 mesh ion-exchange resin in the chloride state and the effluent QCl was titrated for Cl^- by the Volhard method. [d] Micro combustion analysis. [e] See part II.[1c] [f] Slightly hygroscopic. [g] By measurement of the optical density at 350 mμ in 80% methanol solution in comparison with that of standard picric acid solutions.

A. Tetra-n-pentylammonium Bromide. A mixture of 52.13 g. (0.229 mole, b.p. 110–111° at 4.5 mm., $n^{26.5}D$ 1.4339) of tri-*n*-pentylamine, 34.68 g. (0.229 mole, b.p. 129° at 751 mm.) of 1-bromopentane, and 50 ml. of anhydrous acetonitrile was refluxed for 5 days. The cooled, red solution was treated with 500 ml. of diethyl ether and chilled. Filtration of the white solid produced, and washing with ether gave 67.4 g. (0.178 mole, 78%) of tetra-*n*-pentylammonium bromide, m.p. 98.7–99.8°.

B. Di-n-hexyldi-n-heptylammonium Iodide. Di-*n*-heptylamine (35.5 g., 0.167 mole, purified by fractional freezing), 1-iodohexane (70.7 g., 0.334 mole, b.p. 79° at 25 mm.), and 46.5 g. (0.337 mole) of anhydrous potassium carbonate were refluxed together in 470 ml. of absolute ethanol for 7 days. The cooled solution was poured into 1200 ml. of water and extracted with four 50-ml. portions of methylene chloride. The combined, water-washed (one 200-ml. portion) extracts were dried over Linde 5-A molecular sieve, filtered, and evaporated at reduced pressure to 48.1 g. (0.0945 mole, 57%) of di-*n*-hexyldi-*n*-heptylammonium iodide, m.p. 96–97.2°.

C. Tri-n-hexyl-n-heptylammonium Nitrate. A solution of 4.956 g. (1.00 mmole) of tri-*n*-hexyl-*n*-heptylammonium iodide in 50 ml. of ethanol was treated with 1.699 g. (1.00 mmole) of silver nitrate in 10 ml. of ethanol and 2 ml. of water, and the mixture was stirred for 0.5 hr., then filtered. The filtrate was evaporated at reduced pressure to a colorless oil which was crystallized three times from ethyl acetate–diethyl ether, giving 4.036 g. (0.936 mmole, 94%) of tri-*n*-hexyl-*n*-heptylammonium nitrate, white flakes, m.p. 69–70°.

D. Tetra-n-heptylammonium Perchlorate. To a solution of 5.377 g. (1.00 mmole) of tetra-*n*-heptylammonium iodide in the minimum amount of ethanol was added 1.0 ml. of 70% perchloric acid dissolved in 2 ml. of water and 10 ml. of ethanol. The resulting crystals were filtered, washed with water, and redissolved in warm ethanol; 1 ml. of 70% perchloric acid was added, the solution was cooled and filtered, and this precipitation was repeated once more. Two recrystallizations from aqueous ethanol then gave 3.946 g. (0.773 mmole, 77%) of tetra-*n*-heptylammonium perchlorate, white flakes, m.p. 123.5–124°.

E. Tetra-n-pentylammonium Picrate. Tetra-*n*-pentylammonium iodide (10.51 g., 24.7 mmoles) and silver picrate (8.30 g., 24.7 mmoles, obtained on cooling a hot, saturated aqueous picric acid solution in which 1 equiv. of silver oxide had been dissolved[3]) were stirred together in ethanol. The filtered solution was evaporated at reduced pressure to a yellow solid giving 7.212 g. (13.7 mmoles, 55%) of tetra-*n*-pentylammonium picrate after two recrystallizations from ethanol–ether.

F. Tetra-n-pentylammonium Thiocyanate. Tetra-*n*-pentylammonium iodide (4.255 g., 10.0 mmoles) was converted to the perchlorate as previously described. A column of 82 mequiv. of ion-exchange resin in the chloride form (Dowex 1-X4, 50–100 mesh) was converted to the thiocyanate state by treatment with 79.4 g. of potassium thiocyanate in 1 l. of water over a 2-hr. period. The column was washed with 300 ml. of deionized water and 200 ml. of methanol. The tetra-*n*-pentylammonium perchlorate, dissolved in 75 ml. of methanol, was passed through the column during 3 hr., followed by 50 ml. of methanol. Evaporation of the combined effluents at reduced pressure produced a pale yellow oil which crystallized on standing. This was crystallized twice from ethyl acetate at −80°, giving

(3) J. Post and H. Mehrtens, *Ber.*, 8, 1549 (1875).

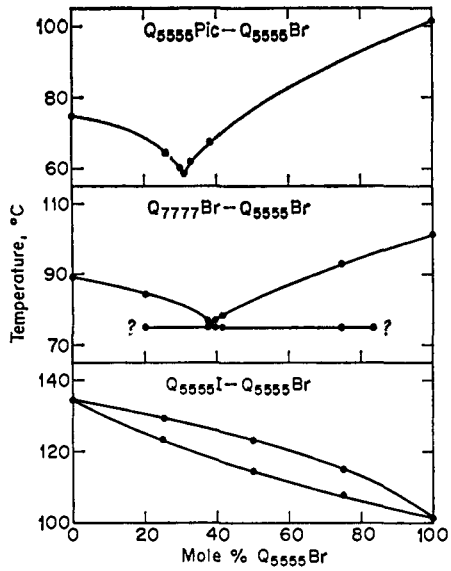

Figure 1. Solid–liquid phase diagrams for three salt–salt systems.

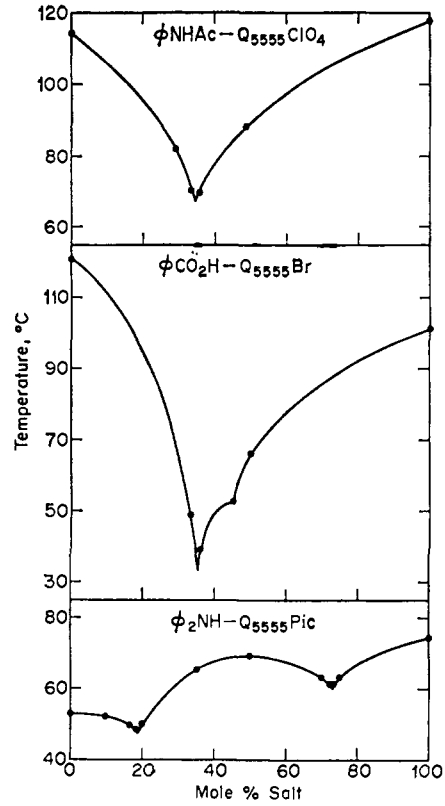

Figure 2. Solid–liquid phase diagrams for three salt–nonelectrolyte systems.

2.66 g. (7.45 mmoles, 74%) of tetra-*n*-pentylammonium thiocyanate as pale yellow flakes.

G. Tri-n-hexyl-n-heptylammonium Bromide. The silver oxide precipitated from 2.549 g. (15.0 mmoles) of silver nitrate in 5 ml. of water by 15 ml. of 1 *N* sodium hydroxide was washed with deionized water and added to a solution of 4.956 g. (10.0 mmoles) of tri-*n*-hexyl-*n*-heptylammonium iodide in 50 ml. of ethanol. The mixture was stirred for 2.5 hr., filtered, concentrated to 25 ml., acidified to pH 2 with 47% aqueous hydrobromic acid, and evaporated at reduced pressure to a colorless oil which crystallized in a vacuum desiccator overnight. Three recrystallizations from ethyl acetate–diethyl ether gave 2.196 g. (4.89 mmoles, 49%) of tri-*n*-hexyl-*n*-heptylammonium bromide.

Freezing Points. A Reichert–Kofler RCH-4065 and an A. H. Thomas 6886-A hot-stage microscope, both operated at 100X magnification, were calibrated on the range 25–150° using a set of ten highly purified compounds whose freezing points, taken from standard compilations, appear to be known to *ca.* ±0.2°. Freezing points were measured as the mean of the two closest temperatures (typically 0.1–0.4° apart) at which pronounced melting and freezing could be observed. Freezing points were reproducible to 0.1–0.2°; results from the two hot stages agreed within 0.3°.

Solid–Liquid Phase Diagrams. The Kofler contact method[4] was used to determine the type of diagram and the transition temperatures for each system. For the several cases which were examined in greater detail, eutectic compositions were determined by fusing successive approximations[5] to the true composition until that was found in which neither component was in excess after fusion at the eutectic temperature. Molecular compounds were identified by preparation of mixtures of various possible stoichiometries, finding that or those which melted sharply without prior melting at a eutectic temperature, and comparing the melting temperature(s) with those observed in the contact preparation. Freezing points of molecular compounds were thus determined to ±0.5°. Eutectic temperatures are considered reliable to about ±1° when determined solely from the contact preparation, but to ±0.5° for the systems shown in Figures 1 and 2. Eutectic composition was fixed to ±1 mole % unit. Other plotted points employed in constructing Figures 1 and 2 were determined by measurement of the temperature of final melting of mixtures of known composition. Note that only the curvature of the diagrams' branches depends upon these less accurate measurements, the salient points of the diagram being fixed by the preceding methods.

Critical Solution Temperatures. These were determined on the hot-stage microscope as the directly observed temperature of disappearance and reappearance of the meniscus on heating and cooling, respectively, the mean being taken as the consolute temperature. The tabulated values are considered accurate to within ±1°.

Charge-Transfer Spectra. Donor nonelectrolytes were recrystallized several times and sublimed at *ca.* 10^{-4} mm. A mixture of the salt and donor was ground together, then fused in a sandwich cell made up of two cylindrical, 10-mm. path, fused-quartz cells filled with triethylene glycol to increase the heat capacity. The liquid film was heated to 10° above the freezing point of the salt and the spectrum was scanned on a Cary Model 14 instrument without heated cell compartment. Spectra could be obtained in this way within 5 min. of the time of first fusion of the mixture. In those cases where very slow decomposition occurred (see Table VIII) the observed transition energies were

(4) L. Kofler and A. Kofler, "Thermo-Mikro-Methoden," Verlag Chemie, Weinheim, 1954, p. 151 ff.

(5) W. C. McCrone, Jr. "Fusion Methods in Chemical Microscopy," Interscience Publishers, Inc., New York, N. Y., 1957, p. 154 ff.

Table II. Reported Melting Points (°C.) of Some Quaternary Ammonium Salts, $R_4N^+X^-$

X	R								
	n-Pr	*n*-Bu	*n*-Am	*i*-Am	*n*-Hex	*n*-Hept	*n*-Oct	*n*-Dec	*n*-Tetradec
I	~280 dec.[a]	146.5[b] 146[c] 145[d] 143.6[e]	134[b]	146.5[e,f] 132[g] 131.8[e]	103.5–104.5[h] 102–103[i]	121–122[i]	127–128[i]	118–120[i]	114.5–115[i]
Br	252[j]	118[c] 117–117.5[k] 115.5[l] 109–110[h] 101.0–101.6[m]	100.0–100.2[m]			88.9–89.1[m]			
ClO_4	237–239[n]	213.3–213.6[o] 213[c] 209.7[p] 208.4[e] 207–209[n] 207[l] 199, 203–204[d]	110–116[n]	119[g] 118[e]	105–106[n]				
Picrate	119.6[q] 117.5–118[j]	90.3[t] 89.5[l,u] 89.4[v]	74[u] 73–74[r] 73–73.5[s]	90[g] 87–87.5[r] 87–87.2[q]					
	117–117.5[r] 115.8[s]	89[s] 86[b]	73[b]	85[l]					
NO_3	260 dec.[r]	120.5–121[r] 119[c,w]	115–115.5[r]	138–131.5[r]					
SCN		126.4–126.9[x]	50.5[y]	106[g] 103.5–104[x] 88[l]					

[a] E. Wedekind, *Ber.*, **35**, 766 (1902). [b] A. A. Vernon and J. P. Masterson, *J. Am. Chem. Soc.*, **64**, 2822 (1942). [c] M. B. Reynolds and C. A. Kraus, *ibid.*, **70**, 1709 (1948). [d] E. D. Hughes, *et al.*, *J. Chem. Soc.*, 1220 (1957). [e] P. Walden and E. J. Birr, *Z. physik. Chem.*, **160**, 57 (1932). [f] W. Ostwald and H. Roederer, *Kolloid Z.*, **82**, 174 (1938). [g] P. Walden and H. Gloy, *Z. physik. Chem.*, **144**, 395 (1929). [h] T. R. Griffiths, *J. Chem. Eng. Data*, **8**, 568 (1963). [i] S. P. Eriksen, L. D. Tuck, and J. F. Oneto, *J. Org. Chem.*, **25**, 849 (1960). [j] S. Sugden and H. Wilkins, *J. Chem. Soc.*, 1291 (1929). [k] P. L. Mercier and C. A. Kraus, *Proc. Natl. Acad. Sci. U. S.*, **42**, 487 (1956). [l] J. A. Geddes and C. A. Kraus, *Trans. Faraday Soc.*, **32**, 585 (1936). [m] J. C. Goodrich, *et al.*, *J. Am. Chem. Soc.*, **72**, 4411 (1950). [n] N. C. Deno and H. E. Berkheimer, *J. Org. Chem.*, **28**, 2143 (1963). [o] Y. H. Inami and J. B. Ramsey, *J. Chem. Phys.*, **31**, 1297 (1959). [p] L. F. Gleysteen and C. A. Kraus, *J. Am. Chem. Soc.*, **69**, 451 (1947). [q] P. Walden, H. Ulich, and E. J. Birr, *Z. physik. Chem.*, **130**, 495 (1927). [r] L. M. Tucker and C. A. Kraus, *J. Am. Chem. Soc.*, **69**, 454 (1947). [s] C. M. French and P. B. Hart, *J. Chem. Soc.*, 1671 (1960). [t] P. Walden and E. J. Birr, *Z. physik. Chem.*, **160**, 45 (1932). [u] C. M. French and D. F. Muggleton, *J. Chem. Soc.*, 2131 (1957). [v] R. P. Seward, *J. Am. Chem. Soc.*, **73**, 515 (1951). [w] D. S. Berns and R. M. Fuoss, *ibid.*, **83**, 1321 (1961). [x] D. T. Copenhafer and C. A. Kraus, *ibid.*, **73**, 4557 (1951). [y] L. C. Kenausis, E. C. Evers, and C. A. Kraus, *Proc. Natl. Acad. Sci. U. S.*, **48**, 121 (1962).

roughly extrapolated back to zero time, except in the case of tetra-*n*-pentylammonium thiocyanate–chloranil which decomposed too rapidly.

The spectra of 1-ethyl-4-carbomethoxypyridinium iodide were obtained in the same manner, the salt having been dried for 20 hr. at 10^{-4} mm. As a check on the integrity of the salt, *Z*-values were measured for methanol (found 83.8; lit.[6] 83.6) and acetone (found, 66.0; lit.[6] 65.7).

Results

The useful temperature range for a fused organic salt is fixed by the freezing point and the stability limit. Hence, the lowest melting materials possible, consistent with reasonable ease of preparation and handling, are desirable. A collection of stable, nonhygroscopic salts representing all of the common anions and with freezing point <100° was the goal of the preparative work.

Table II lists the reported freezing points of previously described quaternary ammonium salts, $R_4N^+X^-$, containing common anions and with R in the range propyl–decyl; it is probably not comprehensive, but it contains most of the known materials of possible interest in the present context.[7] A freezing point minimum in the vicinity of R = hexyl is apparent for the tetra-*n*-alkylammonium salts. The isopentyl salts suggest that branching of the alkyl chains does not lower the freezing point. Attention, therefore, was focused in the first instance on symmetrical and mixed derivatives in the R = *n*-pentyl–*n*-heptyl range. In what follows, a shorthand notation for the quaternary ammonium cations has been adopted: Q_{5555} = tetra-*n*-pentylammonium, Q_{5566} = di-*n*-pentyldi-*n*-hexylammonium, etc.

Freezing Points. Measured freezing points for the present collection of salts are given in Table III. It is seen that all of these anions can now be represented by a salt melting ≤100°. In addition (see following

Table III. Measured Freezing Points of Selected Salts, °C.

Anion	Cation[a]					
	Q_{4444}	Q_{5555}	Q_{6666}	Q_{6667}	Q_{6677}	Q_{7777}
I	146.4	134.6	105.4	95.4	98.9	121.5
Br		101.3	100.8	I 105.0		89.2
				II 86		
				III 57		
ClO_4		117.7	107.2	100.8	104.1	124.2
Pic[b]		74.4				
NO_3		113.9	69.3	71.6		
SCN		I 49.7				
		II 44.5				
NO_2		97.2				

[a] Q_{4444} = tetra-*n*-butylammonium, Q_{6667} = tri-*n*-hexyl-*n*-heptylammonium, etc. [b] Pic = Picrate.

(6) E. M. Kosower, *J. Am. Chem. Soc.*, 80, 3253 (1958).

(7) Many low-melting, nonquaternary salts are also known, and much of the literature of these is to be found in the references of Table II and in the citations of ref. 1d.

Table IV. Data for Binary Solid–Liquid Phase Diagrams

Components 1–2	Melting points, °C.	Diagram type[a]	Eutectic or solid soln. min. melting temp., °C.	Eutectic or solid soln. min. melting composition, mole % 2
$Q_{5555}Pic$–$Q_{5555}Br$	74.4, 101.3	E	58.5	31
$Q_{5555}NO_3$–$Q_{5555}Br$	113.9, 101.3	RIII	100.4	77 ± 3
$Q_{7777}Br$–$Q_{5555}Br$	89.1, 101.3	RV (or E)[b]	75.0	38.5
Acetanilide–$Q_{5555}ClO_4$	114.3, 117.7	E	67.5	34.5
Benzoic Acid–$Q_{5555}Br$	122.5, 101.3, C(1:1) 52.5	[C]	33	35
Diphenylamine–$Q_{5555}Pic$	52.9, 74.4, C(1:1) 69.3	C	47.5[c] 60.0[d]	19[c] 73[d]

[a] E = simple eutectic; RIII, RV = solid solutions of Roozeboom Type III, V; C = congruent melting molecular compound; [C] = incongruent-melting molecular compound. [b] See text. [c] Diphenylamine, molecular compound. [d] Molecular compound, $Q_{5555}Pic$.

section) some eutectic mixtures can provide molten iodide at 89°, molten bromide at 75°, and molten perchlorate at 94°.

$Q_{5555}SCN$ was found to be dimorphic, modification II crystallizing from solution, I generally crystallizing from the melt. On slow heating the solid transition II → I is observed at 40°.

Three polymorphs of $Q_{6667}Br$ were observed. Modification III crystallized from solution; its fusion was observed only on rapid heating. In some preparations the solid transition III → II was observed at 48° on slow heating. Modification II crystallized from the melt, often spontaneously upon fusion of III. I was obtained by very slow heating of larger amounts of III or by seeding the melt.

Solid transitions of $Q_{6666}ClO_4$ were observed at 84.9 and 95.0°; melting points of the other modifications could not be observed. A similar solid transition was observed for $Q_{4444}I$ at 117.7°.

Solid–Liquid Phase Diagrams. The goal of these measurements was not great accuracy, but qualitative and semiquantitative descriptions of the phase diagrams for a large number of systems of varied structure. The Kofler contact method[4] is invaluable for this purpose, yielding the type of diagram and all of the transition temperatures in a single, rapid experiment. In most of the systems studied, no quantitative information on the composition axis of the diagram was obtained. Seven representative systems were studied in greater detail. These are shown in Figures 1 and 2 and/or summarized in Table IV.

A. Salt–Salt Systems. Table V summarizes the observations on 30 salt–salt systems. Part A lists systems whose two components have a common anion. Continuous solid solubility of Roozeboom Type I (linear melting)[8a] or III (minimum melting)[8a] results when the quaternary ammonium cations of the two components differ by no more than one carbon atom. Greater cation differences cause loss of complete miscibility in the solid state, and Roozeboom Type V (quasi-eutectic)[8a] systems result. On the basis of the contact preparation alone, the RV and E systems cannot be distinguished. The designation of systems in Table VA as probably RV follows from the unlikelihood of going from complete to zero solid solubility on adding one carbon atom to a *ca.* 25-carbon cation, and from

(8) (a) Reference 4, pp. 158–163; ref. 5, pp. 146–148; (b) ref. 4, p. 162 ff.

Table V. Binary Solid–Liquid Phase Diagrams for Salt–Salt Systems

System	ΔC atoms[a]	Type of diagram[b]	Eutectic or solid soln. min. temp., °C.
A. Systems with Different Cations			
$Q_{6666}I$–$Q_{6667}I$	1	RIII	92
$Q_{6666}ClO_4$–$Q_{6667}ClO_4$	1	RIII	98.7
$Q_{6666}Br$–$Q_{6667}Br$	1	RI	
$Q_{6666}I$–$Q_{6677}I$	2	RV	91
$Q_{6666}I$–$Q_{5555}I$	4	RV*	91
$Q_{4444}I$–$Q_{5555}I$	4	RV*	111.1
$Q_{5555}I$–$Q_{6667}I$	5	RV*	90.5
$Q_{5555}ClO_4$–$Q_{6667}ClO_4$	5	RV*	93.8
$Q_{5555}I$–$Q_{6677}I$	6	RV*	89
$Q_{5555}I$–$Q_{7777}I$	8	RV*	104
$Q_{5555}Br$–$Q_{7777}Br$	8	RV*	75
B. Systems with Different Anions			
$Q_{5555}I$–$Q_{5555}Br$		RI	
$Q_{7777}I$–$Q_{7777}Br$		RIII	88.5
$Q_{5555}I$–$Q_{5555}ClO_4$		RI	
$Q_{6666}I$–$Q_{6666}ClO_4$		RV*	98
$Q_{7777}I$–$Q_{7777}ClO_4$		RIII	120
$Q_{5555}I$–$Q_{5555}NO_3$		RIII	112.8
$Q_{6666}I$–$Q_{6666}NO_3$		RIII	68
$Q_{6667}I$–$Q_{6667}NO_3$		RIII	67
$Q_{5555}ClO_4$–$Q_{5555}Br$		RIII	97.0
$Q_{5555}ClO_4$–$Q_{5555}SCN(I)$		RIII	48.0
$Q_{5555}ClO_4$–$Q_{5555}SCN(II)$		RIII	43.6
$Q_{5555}Br$–$Q_{5555}NO_3$		RIII[c]	98.5
$Q_{5555}Br$–$Q_{5555}SCN(I)$		RIII	40.3
$Q_{5555}NO_2$–$Q_{5555}I$		RI	
$Q_{5555}NO_2$–$Q_{5555}ClO_4$		RIII	94
$Q_{5555}NO_2$–$Q_{5555}Br$		RIII	92.3
$Q_{5555}Pic$–$Q_{5555}I$		E[d]	71.8
$Q_{5555}Pic$–$Q_{5555}Br$		E[c,d]	61.3
$Q_{5555}Pic$–$Q_{5555}NO_3$		E[d]	60.3
$Q_{5555}Pic$–$Q_{5555}SCN(II)$		E[d]	35.0

[a] ΔC atoms = difference in total number of carbons in the two cations of the system. [b] E = simple eutectic diagram; RI, RIII, etc. = solid solution diagrams of Roozeboom Type I, III, etc.; RV* = probably Roozeboom Type V solid solution, but not distinguishable from simple eutectic by this experiment alone; see text. [c] Supplementary X-ray powder data. [d] The RV alternative is considered less likely, as $Q_{5555}Pic$ (different habit, greater density than all other Q^+X^- studied) appears to crystallize in a different system.

evidence of extensive (>30%) partial solid solubility in the system $Q_{6666}I$–$Q_{6677}I$. Since we were not prepared to measure X-ray powder patterns at other than room temperature this evidence comes from hot-stage microscopy of mixtures toward the extremes of

Table VI. Binary Solid–Liquid Phase Diagrams for Salt–Nonelectrolyte Systems

A. Diagram type[a] and transition temperatures[b]					
	Salt				
Nonelectrolyte[c]	$Q_{5555}Br$	$Q_{5555}I$	$Q_{5555}ClO_4$	$Q_{5555}SCN$	$Q_{5555}Pic$
Eicosane (36)	I	I	I	I	I
Bibenzyl (51)	E(50.5)		I		E(42)
Fluorene (115)	E(81)		E(88)		E(52)
Azulene (99)	E(68)				E(42)
Acetanilide (114)	C(44.5)	E(61)	E(68)		E(41)
Benzoic acid (121)	C(55)		E(82)		E(34)
Cholesterol (148)	C(110.5)	E(118)	E(114)	E(43)	
p-Nitrophenol (113)	C(25)				
Hydroquinone (172)	C_1(53.5)		E(58)		C_1(47.8)
	C_2(76.5)				C_2(49)
	[C_3(81)]				
Imidazole (89)	E(22)				E(37)
Urea (133)	E(74)		E(108)		
Myristic acid (54)	E(36)				
Diphenylamine (53)	[C_1(50.5)]				C(69.3)
	C_2(61)				
Picric acid (122)					E(40)
1,3,5-Trinitrobenzene (122)	E(72)[d]	D[d]	E(82)	E(34)[d]	
2,4-Dinitrobromobenzene (72)	E(45)		E(64)		
Diethylbenzalmalonate (50)	E(45)			E(24)	
Benzil (95)		E(63)[e]			

B. Systems forming molecular compounds	
System	Phases present[a] and transition temperatures (°C.)
Benzoic acid–$Q_{5555}Br$	(a) $C_6H_5CO_2H$ (121), E (33), C(1:1, incongruent) (52.5), $Q_{5555}Br$ (101)
	(b) $C_6H_5CO_2H$ (121), E (39), C′(?, not 2:1, congruent) (54), E (48), $Q_{5555}Br$ (101)
Acetanilide–$Q_{5555}Br$	C_6H_5NHAc (114), E (39), C(?, congruent) (44.5), E (35), $Q_{5555}Br$ (101)
Hydroquinone–$Q_{5555}Br$	(a) $C_6H_4(OH)_2$ (172), C_3(3:1, incongruent) (81), E(75), C_2(2:1, congruent) (76.5), E (49.5), C_1(?, not 1:1, congruent) (53.5), E (39), $Q_{5555}Br$ (101)
	(b) $C_6H_4(OH)_2$ (172), C_3(3:1, incongruent) (81), E(75), C_2(2:1, congruent) (76.5), E (49.5), $Q_{5555}Br$ (101)
	(c) $C_6H_4(OH)_2$ (172), C_3(3:1, incongruent) (81), E (75), C_2(2:1, congruent) (76.5), E (46.5), C′$_1$(?, not 1:1, congruent) (54.5), E (52), $Q_{5555}Br$(101)
Cholesterol–$Q_{5555}Br$	ROH (148), E (102), C(3:2, congruent) (110.5), E (92), $Q_{5555}Br$ (101)
p-Nitrophenol–$Q_{5555}Br$	ArOH (113), E (16), C(?, congruent) (25), E (1), $Q_{5555}Br$ (101)
Hydroquinone–$Q_{5555}Pic$	$C_6H_4(OH)_2$ (172), E (47), C_2(1:1, congruent) (49.0), E (44), C_1(2:1, congruent) (47.8), E (45.5), $Q_{5555}Pic$ (74.4)
Diphenylamine-$Q_{5555}Pic$[f]	

C. Benzoic acid–variable QBr systems			
	Transition temperature (°C.)		
QBr, m.p. (°C.)	E_{ArCO_2H-C}	C	E_{C-QBr}
$Q_{5555}Br$ (101)	39	54	48
$Q_{6666}Br$ (101)	42	59	49
$Q_{7777}Br$ (89)	29	32	26

D. Acetanilide–variable QI systems			
	Salt, m.p. (°C.)		
	$Q_{5555}I$ (135)	$Q_{6666}I$ (105)	$Q_{7777}I$ (122)
Diagram type (eut. temp.)	E (61)	E (32)	E (49)

[a] E = eutectic diagram, C = congruent-melting molecular compound, [C] = incongruent-melting molecular compound, I = incomplete liquid–liquid miscibility at the freezing point—no apparent freezing point depression, D = mixture decomposes. [b] Melting point or peritectic temperature of molecular compounds, eutectic temperature for E-type systems given in parentheses. [c] Melting point in parentheses. [d] Red melt, color disappears on crystallization. [e] For $Q_{6667}I$. [f] See Table IV.

composition where, in the RV case, no eutectic melt is observed beyond the solid solubility limits. Indications of partial solid solubility were also obtained for the system $Q_{5555}Br$–$Q_{7777}Br$, but due to the difficulties of detecting small amounts of liquid at the composition extremes the solidus curve of Figure 1b could not be reliably determined. X-Ray powder patterns obtained at room temperature confirmed the absence of diffraction maxima due to either pure component in the system $Q_{5555}Br$–$Q_{5555}NO_3$. In the systems $Q_{5555}Br$–Q_{5555}picrate (hereafter Pic) and $Q_{5555}Br$–$Q_{7777}Br$ the room temperature powder patterns of intermediate compositions showed only maxima differing undetectably from those of the pure components.

Part B of Table V contains the anion-variable systems, whose behavior can be summarized as follows. All combinations among the anions studied give continuous solid solubility, usually of the minimum melting (Roozeboom Type III) variety, with two exceptions. The first is that the picrates give simple eutectic diagrams with the salts of the inorganic ions. The other exception is the system $Q_{6666}I$–$Q_{6666}ClO_4$, in which solid solubility is incomplete, probably a case of isodimorphism.[8b]

B. Salt–Nonelectrolyte Systems. Table VI presents results for 50 binary systems. These display a rich variety of phenomena. The composition of the molecular compounds observed was in most cases de-

termined; these systems are described in part B of the table. Parts C and D of Table VI show the effect of structure variation in Q on two types of system.

An interesting result from Table VI is the fact that the quaternary ammonium salts in the pentyl–heptyl range are, in the liquid state, miscible in all proportions with most organic nonelectrolytes except saturated hydrocarbons. This prompted a wider study of liquid–liquid miscibilities which is described in a later section. The large freezing point depressions observed in Table VI make it generally possible to make measurements on such systems, or conduct chemical reactions in them, at temperatures well below the freezing point.

C. Molecular Compounds. Failure of the same phases to nucleate in different preparations of a given system gave rise to substantial variability in the nature of the phase diagrams observed. In the system hydroquinone–$Q_{5555}Br$ (Table VIB) two variations were observed in which the most salt-rich compound, C_1, was either missing (system b) or replaced by a different, congruent-melting compound, C_1', m.p. 54.5° (system c). The system benzoic acid–$Q_{5555}Br$ consistently gave diagram b of Table VIB in contact preparations. However when larger scale mixtures of various stoichiometries were prepared in order to determine the stoichiometry of the congruent-melting molecular compound of m.p. 54°, a mole ratio of 1:1 produced instead a new incongruently melting compound, m.p. 52.5, and this material was used to construct the diagram shown in Figure 2. Mixtures of 2:1 composition produced no compound, and the original 54° compound is probably also 1:1.

In the system acetanilide–$Q_{5555}Br$, mixtures containing 50 and 40 mole % QBr displayed the 35° eutectic; mixtures containing 33.3, 25, and 20% QBr displayed the 39° eutectic. The stoichiometry is therefore complex, falling between 3:2 and 2:1.

Those nonelectrolytes with which QBr forms compounds have in common the property of being hydrogen-bonding proton donors. Since bromide ion is known to form strong hydrogen bridges in solution,[9] it seems likely that hydrogen bonding is the source of interaction leading to these molecular compounds in the solid state. The crystal structure of an analogous compound, $(C_2H_5)_4NBr{\cdot}2$ succinimide, has been studied[10] and consists of sheets of hydrogen bonded complex anions of the type $>NH\cdots Br^-\cdots HN<$ alternating with parallel cation layers. Infrared spectra of the solid compounds of Table VI were determined and are summarized in Table VII in comparison with those of the parent compounds.

The spectra of the QBr–HA compounds show marked changes in bands associated with the proton motions. In the benzoic acid–QBr compound spectrum (Figure 3), consolidation of the highly structured $\nu_s(OH)$[11] of solid benzoic acid into a broad band centered on 2830 cm.$^{-1}$ implies breakup of the ArCOOH dimer structure and is consistent with an $ArCOOH\cdots Br^-$ bridge in the complex. The shift of $\nu_s(C{=}O)$ from

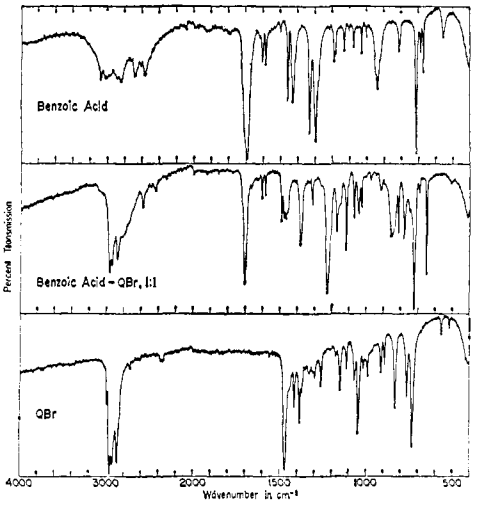

Figure 3. Infrared absorption spectra of solid phases in the system benzoic acid–tetra-*n*-pentylammonium bromide, measured as Nujol–halocarbon mulls.

1693 to 1703 cm.$^{-1}$ is consistent with such a structure change and rules out a linear $-OH\cdots O-$ bridging chain structure in which $\nu_{C=O}$ would be expected to shift markedly to lower frequency.[12] The coupled $\nu_s(C{-}O)$ and $\nu_b(OH)$ bands observed at 1429 and 1298 cm.$^{-1}$ (lit.[13] 1420 and 1287 cm.$^{-1}$) in solid benzoic acid are probably best identified with those at 1382 and 1227 cm.$^{-1}$ in the complex. This shift is in the direction of unbonding.[11] The out-of-plane bending motion $\nu_t(OH)$ at 939 cm.$^{-1}$ (lit.[13] 935 cm.$^{-1}$) also shifts in the direction of unbonding, to 850 cm.$^{-1}$ in the molecular compound. Thus it appears likely that the structural unit of the compound is $ArCO_2H\cdots Br^-$ in which the hydrogen bridge is slightly weaker than those of the solid acid dimer.

Without speculating on possible assignments of the highly coupled OH bending modes in the case of hydroquinone (HQ) and its molecular compounds, it is interesting to note the close similarity of the shifts occurring with Q^+Br^- and Q^+Pic^- as the second component. In each case the complex band structure at 1260–1150 cm.$^{-1}$ simplifies on compound formation to three well-defined bands near 1270, 1250, and 1200 cm.$^{-1}$, and the 1480-cm.$^{-1}$ absorption is replaced by a pair of bands near 1486 and 1460 cm.$^{-1}$. In view of the considerable differences between Br^- and Pic^-, this similarity implies that the spectral changes stem principally from breakdown of the complex hydrogen-bonded structure of crystalline HQ.

$Q_{5555}I$ appears to form no compounds of this sort.[14] Powell and Wait[10] attribute the absence of a $Q_{2222}I$–succinimide compound to geometric factors. However, iodide is a weaker hydrogen-bonding proton acceptor[9] than bromide and this may be the predominant factor.

Preliminary experiments showed that potentially useful proton magnetic resonance spectra can be

(9) A. Allerhand and P. von R. Schleyer, *J. Am. Chem. Soc.*, **85**, 1233 (1963).

(10) H. M. Powell and E. Wait, *J. Chem. Soc.*, 1866 (1958).

(11) Nomenclature follows G. C. Pimentel and A. L. McClellan, "The Hydrogen Bond," W. H. Freeman and Co., San Francisco, Calif., 1960, Chapter 3.

(12) S. Bratož, D. Hadži, and N. Sheppard, *Spectrochim. Acta*, **8**, 249 (1956).

(13) D. Hadži and N. Sheppard, *Proc. Roy. Soc.* (London), **A216**, 247 (1953).

(14) Absence of a molecular compound simply because the solid phase fails to nucleate is always a possibility, although a less likely one where a series of systems is studied.

Table VII. Infrared Spectra of Molecular Compounds[a]

A		B		
$C_6H_5CO_2H$	$C_6H_5CO_2H$–QBr (1:1)	$(C_7H_6)_2NH$	$(C_6H_5)_2NH$–QPic (1:1)	QPic
3000 m, b		3408 w	3290 m	
2890 m, b	2830 m, b	3385 w	3195 w	
2840 m, b	2750 sh	3039 w	3125 w	
2680 m, b			3056 w	
2610 m	2585 w	1597 s	1630 s	1629 s
2575 m		1589 s	1604 s	1609 m
		1583 s	1591 s	1559 m, s
1693 s	1703 s[b]	1521 s	1567 s	1494 m
1456 m	1492 w	1497 s	1559 sh	
1429 m	1479 w		1540 m	
1330 s	1454 w		1500 s	
1298 s	1382 m		1480 m	
	1312 w			
	1227 s	1460 m	1470 m	1467 w
			1461 w	
939 m, b	850 m, b			
	781 m	1420 m	1432 m, w	1438 m, w
672 m, w	652 m, s	1243 w		
559 w		1173 w	1178 m, w	1161 m
		1160 w	1162 m, w	
		1150 m		
		1086 w	1080 m, w	1075 m
		1075 w	1043 w	1045 w
		1023 w	1030 w	
		879 m		

C			D			
Hydroquinone	Hydroquinone–QBr (2:1)	Hydroquinone–QBr (1:1)	Hydroquinone	Hydroquinone–QPic (1:1)	Hydroquinone–QPic (2:1)	QPic
3270 b, s	3300 b, s	3385 b, s[b]	3270 b, s	3500 m, b	3230 m, b	
	3210 b, s	3315 b, s[b]		3220 m, b		
1521 s	1520 s	1520 s				
1480 s	1486 m	1461 s	1521 s	1519 m, s	1520 m, s	
	1461 s		1480 s	1487 m	1481 m	1494 m, w
				1458 m	1462 m	1438 m, w
1262 m	1270 w	1270 w		1430 m	1432 m	
1247 s	1250 m	1248 m	1359 w	1362 m	1365 m	1363 m
1224 sh	1208 s	1207 s		1333 s	1338 s	1331 m
1214 vs				1320 s	1321 s	1310 s
1198 s						
1167 w			1262 m	1263 s	1269 s	1267 m, s
1100 m	1097 w	1098 w	1247 s	1247 s	1250 m	
850–600 vb		1091 w	1224 sh		1238 sh	
			1214 vs			
811 w			1198 vs	1186 m	1200 m	
			1167 w	1160 m	1162 m	1160 m
745 sh	740 w	731 w				
707 w	732 w		1100 m	1091 w		
620 w, b	601 w, b	601 w, b	1012 w			
			832 s	831 m	839 m	
			810 w	789 m	791 m	
			762 s	760 m	760 w	

[a] Measured in halocarbon oil and Nujol mulls: w = weak, m = medium, s = strong, vs = very strong, b = broad, sh = shoulder, vb = very broad. Bands which appeared identical in the parent and molecular compounds were not tabulated. Frequency in $cm.^{-1}$. [b] Significantly narrower than in the parent compound.

measured in the molten salt medium, although a line width of ~5 c.p.s. was observed, presumably due to viscosity broadening in the melt near the freezing point. Spectra of the *p*-nitrophenyl-$Q_{5555}Br$ system at 107° showed downfield shifts of the OH proton in excess of 2 p.p.m. attributable to $ArOH\cdots Br^-$ hydrogen bridges.

Binary systems containing QPic provide a source of information on the electron acceptor capability of the picrate ion. One would expect this to be very much less than that of picric acid due to the added unit negative charge. It is in fact found that $Q_{5555}Pic$ forms no compounds[14] with azulene, fluorene, or bibenzyl, all of which give compounds with 1,3,5-trinitrobenzene[15–17] and with picric acid.[16,18,19] On the other hand, $Q_{5555}Pic$ does form compounds with the donor molecules diphenylamine and hydroquinone which possess strongly electron-releasing substituents.

(15) M. Gordon, *Chem. Rev.*, **50**, 172 (1952).
(16) A. Kofler, *Z. Elektrochem.*, **50**, 200 (1944).
(17) R. L. Letsinger and I. H. Skoog, *J. Am. Chem. Soc.*, 77, 5176 (1955).
(18) We have observed a congruent-melting compound, m.p. 133.6°, in azulene–picric acid contact preparations.
(19) R. Foster, D. L. Hammick, and S. F. Pearce, *J. Chem. Soc.*, 244 (1959).

In view of the fact that QPic forms no compounds[14] with benzoic acid, acetanilide, or picric acid, it is unlikely that hydrogen bridge formation to picrate ion as proton acceptor is the only interaction in these compounds. Nevertheless, the infrared results (Table VIIB and D) show that formation of the compounds is attended by hydrogen bonding *changes*, and at least in the case of diphenylamine probably by formation of a stronger hydrogen bridge. It is likely that the energetics of the formation of these compounds involves donor–acceptor interaction, hydrogen bonding, and crystal-packing considerations.[20]

Acceptor–X^- Charge-Transfer Complexes in Molten Q^+X^-. 1,3,5-Trinitrobenzene (TNB) forms rather stable, colored complex ions with a variety of donor anions.[21] Those (covalent) complex salts derived from the more basic donors (OR^-,[22] CN^-,[23] SO_3^{2-}[24]) are isolable in the solid state. Those (charge-transfer) complexes derived from the more polarizable donors (I^-, Br^-, SCN^-) have been studied in solution in detail by Briegleb, Liptay, and Fick.[25] It was thus of interest to determine the Q^+X^-–TNB phase diagrams to determine if the compounds with QI, QBr, and QSCN could be observed in the solid state. Molten mixtures of TNB with these QX are indeed highly colored; however, in each of many trials the color disappeared on crystallization. The contact preparation shows a simple eutectic system (Table VI). Whether $Q^+X\cdot TNB^-$ is unstable in the solid or is simply failing to nucleate is not known.

Using the lowest melting available QX, it was possible to measure the electronic spectra of these complex ions in thin films of the molten salt. Results for the acceptors chloranil and 9-nitroanthracene as well as for TNB are given in Table VIII.

Table VIII. Charge-Transfer Spectra in Molten QX[a]

Acceptor	Salt			
	$QClO_4$[b]	QBr[c]	QSCN[d]	QI[e]
1,3,5-Trinitrobenzene	*f*	378 (26.4)	411 (24.3)	342[g], 482[h] (29.8, 20.7)
9-Nitroanthracene	349	350		
	366	367		
	385	385		
Chloranil	~365[i,j]	476 (21.0)	*k*	
	296[j]			

[a] Wavelength, mμ (frequency, $cm.^{-1} \times 10^{-3}$). [b] Q_{6666}. [c] Q_{7777}. [d] Q_{5555}. [e] Q_{6667} and Q_{6667}–Q_{6666} mixtures. [f] Below cutoff wave length (250 mμ) of this cell assembly. Solution (ethanol) spectrum λ_{max} 225 mμ: P. Fielding and R. J. W. LeFèvre, *J. Chem. Soc.*, 2812 (1950). [g] Shifts with time to 476 mμ. [h] Shifts with time to 353 mμ. [i] Shoulder. [j] Solution in inert solvents: λ_{max} 282, 369 mμ.[25c] [k] Decomposes immediately.

If the structures of the two classes of TNB–donor anion complexes are correctly given[25a,b,26] as

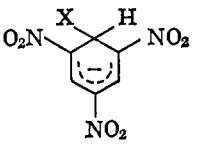

I, $X = OR^-, CN^-, SO_3^{2-}$

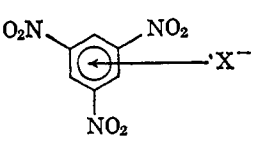

II, $X = I^-, Br^-, SCN^-$

the acceptor properties should reside in differentiable structural features occurring to a certain extent coincidentally together in TNB. Suitably modified acceptors should thus exist which are capable of giving Meisenheimer[22] adducts (I) but not charge-transfer complexes (II). One such acceptor has been found in 9-nitroanthracene which gives a compound with sodium ethoxide[22] but whose electronic spectrum is essentially identical in solution,[27] in molten $QClO_4$, and in molten QBr.

Comparison of the transition energies for Q^+-TNB·X^- in molten Q^+X^- with those determined in a variety of solvents yields some information on medium effects present in the molten salt. In each of the four systems studied the charge-transfer transition energy is smaller in the fused salt than in any solvent; this information is summarized in Table IX. Briegleb, Liptay, and Fick found no correlation of ν_{CT} with dielectric constant or with Kosower's[6] *Z*-values. It is likely that specific interaction of X^- with the medium is greater with the TNB·X^-, etc., complexes than with the ion-pair pyridinium $^+X^-$ complexes from which the *Z*-scale derives. A reasonable qualitative chemical correlation of ν_{CT} with increasing X^-–medium interaction can be arrived at in the following way. Electronic excitation results in a more diffuse electron distribution and a shift in the center of charge of the complex anion. Electrostatic interactions of X^- with the medium are thus partly lost in the excited (Franck–Condon) state, and this loss (and hence the excitation energy) will be greater the greater the original ground-state electrostatic interactions of X^- with solvent dipoles or counterions. Since the nucleophilic reactivity of X^- is known to be attenuated by these same interactions,[28,29] one is led to expect a correlation of ν_{CT} with decreasing X^- nucleophilicity. Although a single scale of comparative rate data is not available for this range of media, one can qualitatively order the media with respect to X^- interaction, taking dipolar aprotic solvents as a norm and considering that solvent hydrogen bonding to, and ion association of, X^- are the principal additional deactivating interactions.[28,29] The general order of X^-–medium interactions predicted on this basis corresponds to the orders of increasing ν_{CT} of Table IX. Thus OH proton donor solvents which strongly solvate X^- by hydrogen bonding produce the highest excitation energies; this is also true[1c,9] to a lesser extent for chloroform, which appears at somewhat lower ν_{CT}. Although the highly dipolar, aprotic solvents (dimethyl sulfoxide, acetonitrile, acetone) are somewhat erratic in behavior, they produce generally higher excitation energies than do the very poorly

(20) The first two of these interactions may be contributing to the stability of the "dipole solvate between the picrate ion and *p*-nitroaniline" whose existence A. D'Aprano and R. M. Fuoss, *J. Phys. Chem.*, 67, 1871 (1963), deduced from conductance measurements on Q_{4444}Pic in *p*-nitroaniline–dioxane.

(21) L. J. Andrews and R. M. Keefer, "Molecular Complexes in Organic Chemistry," Holden-Day, Inc., San Francisco, Calif., 1964, pp. 138, 148 ff.

(22) J. Meisenheimer, *Ann.*, 323, 305 (1902).

(23) C. L. Jackson and R. B. Earle, *Am. Chem. J.*, 29, 89 (1903).

(24) R. A. Henry, *J. Org. Chem.*, 27, 2637 (1962).

(25) (a) G. Briegleb, W. Liptay, and R. Fick, *Z. physik. Chem.* (Frankfurt), 33, 181 (1962); (b) *Z. Elektrochem.*, 66, 851 (1962); (c) *ibid*, 66, 859 (1962).

(26) L. K. Dyall, *J. Chem. Soc.*, 5160 (1960).

(27) R. N. Jones, *Chem. Rev.*, 41, 353 (1947).

(28) A. J. Parker, *Quart. Rev.* (London), 16, 163 (1962).

(29) J. F. Bunnett, *Ann. Rev. Phys. Chem.*, 14, 281 (1963).

Table IX. Medium Dependence of Charge-Transfer Band Frequencies, ν_{CT} (cm.$^{-1}$ × 10^{-3})[a]

Complex	Solvent order
TNB·I^{-}[b]	Fused salt (20.7) < THF[c] (21.1) < acetone (21.2) < CCl_4 (21.4) < $C_6H_5CF_3$ (21.6) < DMSO[d] (22.4) < CH_2Cl_2 (22.6) < $CHCl_3$ (23.0) < CH_3CN (23.1) < *t*-BuOH (23.5) < *i*-PrOH (25.0)
TNB·Br^{-}[e]	Fused salt (26.4) < DMSO (26.7) < acetone (30.6) < THF (30.7) < glyme[f] (31.0) < CH_3CN (31.3) < *i*-PrOH (34.2)
TNB·SCN^{-}[g]	Fused salt (24.3) < CH_3CN (28.4)
TCNE·Br^{-}[h]	CH_3CN (21.7) < acetone (21.9) < DMSO (22.2) < glyme (22.8) < THF (22.9)
Chloranil·Br^{-}[e]	Fused salt (21.0) < CH_3CN (23.1) = acetone < glyme (24.2) < THF (24.4)

[a] From ref. 25 and Table VIII. [b] $Q_{5555}I$ in solution. [c] Tetrahydrofuran. [d] Dimethyl sulfoxide. [e] Lithium bromide. [f] Ethylene glycol dimethyl ether. [g] Ammonium thiocyanate. [h] Tetracyanoethylene–lithium bromide.

polar solvents in the system $R_4N^+I^-$–TNB. In the systems LiBr–acceptor, where Li^+,Br^- ion pairing is much more important, the reverse behavior is observed, enhanced excitation energies resulting from the stronger electrostatic interactions of ground state X^- in the poorly polar solvents. This is quite analogous to the observed effects on X^- nucleophilicity.[30]

The low values of ν_{CT} observed for the fused Q^+X^- are consistent with a picture of these melts as media in which stabilizing X^- interactions have been minimized. Conductance measurements on molten Q^+X^- of this type characterize them as liquids consisting essentially of free ions.[31,32] Consideration of simple electrostatic models for the charge-transfer complex suggests that the principle difference in medium effect on ν_{CT} between molten Q^+X^- and simple dipolar nonelectrolytes lies in the large cation size. We will return in a later section to the importance of this parameter for other properties of the liquid Q^+X^-.

From the viewpoint of correlation of increasing nucleophilicity of X^- with decreasing ν_{CT}, the results are most interesting in their prediction of an unusually high level of nucleophilic reactivity for molten Q^+X^-. Although some unusual reactions of anions in these media have been discovered,[1a] a kinetic test of this prediction has not yet been undertaken.

Mutual Solubility with Liquid Nonelectrolytes. In order to obtain needed information on the solvent properties of these melts for nonelectrolytes as a function of structure and to learn something more about the interactions present in the salt–nonelectrolyte systems, the critical solution behavior with a variety of liquid nonelectrolytes was observed by hot-stage microscopy. Table X contains information of this sort for tetra-*n*-pentylammonium picrate paired with 26 liquids.

If the liquids are arranged in order of decreasing hydrophilic and increasing lipophilic character, as has been done approximately in Table X, it is seen that the mutual solubility with the quaternary picrate is small at either end of the scale and passes through a maximum in the center where complete liquid–liquid miscibility with aromatic and halogenated hydrocarbons and dipolar aprotic liquids is the rule. The same general pattern, qualitatively varying and overlaid with other effects, is observed with the other salts as well. Table XI contains comparative data for six tetra-*n*-pentylammonium salts with a smaller selection of nonelectrolytes.

Table X. Critical Solution Temperatures for Q_{5555} Picrate–Liquid Nonelectrolyte Systems

Liquid	C.s.t., °C.[a]
Water	>100
Glycerol	>210
Urea	>150
Diethanolamine	147
Ethylene glycol	145
Formamide	116
Ethanolamine	98
1,4-Butanediol	88
Propylene glycol	70
Diethylene glycol	M
Tetradecanol	43
Decanol	M
1-Cyanodecane	M
Decylamine	M
Acetonitrile	M
N,N-Dimethylformamide	M
Dimethyl sulfoxide	M
Azobenzene	M
Azulene	M
1,1,2,2-Tetrachloroethane	M
1,2,3,4-Tetrahydroisoquinoline	M
Fluorene	M
1,2-Diphenylethane	132
Propylbenzene	>140
t-Butylbenzene	>145
Tri-*n*-butylamine	>175
1,5,9-Cyclododecatriene	>200

[a] M = miscible in all proportions at the lowest attainable liquid temperature, usually ~10° below the freezing point.

From these data one arrives at the order $Pic^- < ClO_4^- < NO_3^-$, $SCN^- < Br^-$, I^- for increasing mutual solubility of the molten salts with nonelectrolytes at the nonpolar end of the scale. This is approximately the order of increasing polarizability. The miscibility order with respect to the highly polar, hydroxylic liquids is $Pic^- < ClO_4^- < SCN^- < I^- < NO_3^- < Br^-$, which evidently reflects a contribution of specific anion solvation by the nonelectrolyte through hydrogen bridging. This is closely similar to the order of increasing preferential solvation of the anions by water in 50% dioxane observed by Grunwald, Baughman, and Kohnstam[33]: ClO_4^- < 2-naphthalenesulfonate < $I^- < NO_3^- < Br^-$. The position of picrate, the only organic anion studied, seems anomalous in the first sequence (as contrary to the idea of like dissolving like)

(30) S. Winstein, L. G. Savedoff, S. Smith, I. D. R. Stevens, and J. S. Gall, *Tetrahedron Letters*, No. 9, 24 (1960).
(31) R. P. Seward, *J. Am. Chem. Soc.*, 73, 515 (1951).
(32) L. C. Kenausis, E. C. Evers, and C. A. Kraus, *Proc. Natl. Acad. Sci. U. S.*, 48, 121 (1962); 49, 141 (1963).
(33) E. Grunwald, G. Baughman, and G. Kohstam, *J. Am. Chem. Soc.*, 82, 5801 (1960).

Table XI. Critical Solution Temperatures for $Q^+_{5555}X^-$–Liquid Nonelectrolyte Systems

Nonelectrolyte	C.s.t., °C.[a] I^-	Br^-	SCN^-	NO_3^-	ClO_4^-	Pic^-
Glycerol	135	62	150	100	>200	>210
Diethanolamine	M		M		112.5	147
Ethylene glycol	M		36	M	100	145
Formamide					M	116
Ethanolamine		M		M		98
Propylene glycol		M				70
N,N-Dimethyl-formamide	M	M		M		M
Dimethyl sulf-oxide	M	M	M	M	M	M
p-Nitrotoluene	M	M		M		
1,2-Diphenyl-ethane	M	M	M	M	121	132
n-Butylbenzene		M		M		>145
2-*t*-Butylnaph-thalene–eico-sane (4:1)	M	M	>185	>150		
Eicosane		>200				

[a] M = miscible at lowest accessible liquid temperature, generally ~10° below the freezing point of the salt.

as well as in the second where some promotion of its miscibility by its hydrogen bridging capabilities (as shown in the stoichiometry of picric acid–base equilibria in nonwaterlike solvents,[34] in the added stability of $R_3NH^+\cdots Pic^-$ ion pairs,[35] and in the spectra of Q^+-Pic^- molecular compounds in Table VII) might be expected.

Table XII. Critical Solution Temperatures for Three Nonelectrolytes with Various Salts, Q^+X^-

System	C.s.t., °C.[a] Q_{5555}	Q_{6666}	Q_{6667}	Q_{6677}	Q_{7777}
1,2-Diphenylethane–$Q^+ClO_4^-$	121	M	M	M	M
Ethylene glycol–Q^+-ClO_4^-	100	132	143.5	146.5	142
Glycerol–Q^+I^-	135	190	>195	>195	>195

[a] M = miscible at the lowest accessible liquid temperature, generally ~10° below the freezing point of the salt.

The effect of cation structure on the mutual solubility is illustrated in Table XII. Increasing the hydrocarbon chain length in the cation generally increases miscibility with the hydrocarbon and decreases miscibility with the polar nonelectrolytes, as expected. The maximum in the critical solution temperature in the $Q^+ClO_4^-$–ethylene glycol system (which corresponds closely to the freezing point minimum for the $Q^+ClO_4^-$, whether coincidentally or reflecting some regularity in the liquid Q^+X^- structure) is less simply accounted for.

Discussion

Liquid State. The failure of the miscibility with nonelectrolytes of Q^+X^-, as ionic liquids, to increase indefinitely with increasing polarity of the nonelectrolyte is contrary at first glance to common generalizations. Incomplete liquid–liquid miscibility corresponds to large positive deviations from Raoult's law. Stabilizing, specific QX–nonelectrolyte interactions (solvation), which would lead to negative deviations, are evidently overwhelmed by other forces.[36] Large positive deviations from Raoult's law ordinarily result from large differences in the cohesive energies (internal pressures) of the two pure liquids.[37] Of the various approximate measures which can be employed in ranking the cohesive energy densities of liquids, three have been found which could be applied to the molten Q^+X^- at hand. With two of these, representative molten inorganic salts can also be added to the list. The results are given in Table XIII. This is predominantly an order of increasing polarity.

Table XIII. Values for Several Liquids of Three Measures of the Cohesive Energy Density

Liquid	Temp., °C.	$\gamma/V^{1/3}$, dyne cm.$^{-2}$[a]	$\Delta E_{vis}/V$, cal. cm.$^{-3}$	Z, kcal.
n-Pentane	20	3.28[b]	13.7[c,d]	60.1[e]
Ethyl ether	20	3.60[b]	15.5[c,d]	
Acetone	20	5.57[c]	20.7[c,d]	65.7[e]
QI	*f*	4.2[g]	38[h]	66.4[i]
$QClO_4$	*f*	4.4[g]	31[h]	66.9[i]
QPic	*f*	5.0[g]	18[h]	
Benzene	20	6.51[b]	28.6[c,d]	
Acetonitrile	20	7.77[c]		71.3[e]
Nitromethane	20	9.80[c]	33.7[c]	
Ethylene glycol	20	12.5[c,j]	139[c]	85.1[e]
Glycerol	20	15.1[c,j]	185[c,k]	
CsI	821	17[l,m]		
KBr	800	26[l,m]	120[l]	
Water	20	27.7[j]	236[d]	94.6[e]
NaCl	1000	34[l,m]	292[l]	

[a] $\gamma/V^{1/3}$ is a not very sensitive function of the radius ratio when computed for molten salts. The known radii for the inorganic ions were employed, together with the following values of the radius ratio for Q^+I^-, $Q^+ClO_4^-$, and Q^+Pic^- derived from r_Q = 5.0 Å. and the relative molar volumes of liquid Q^+I^- and Q^+Pic^-: 2.32, 2.50, 1.42. [b] Reference 38. [c] J. Timmermans, "Physico-Chemical Constants of Pure Organic Compounds," Elsevier Publishing Co., Amsterdam, 1950. [d] R. H. Ewell and H. Eyring, *J. Chem. Phys.*, **5**, 726 (1937). [e] Reference 6. The selection of liquids in this table gives the impression that a smooth correlation of Z with the other measures of internal pressure exists; it is in fact smooth only for hydroxylic liquids. [f] $\gamma/V^{1/3}$, 153°. $\Delta E_{vis}/V$, ~150°. Z, f.p. ±5°. [g] Q_{5555}. [h] Tetraisopentylammonium salts; data of P. Walden and E. J. Birr, *Z. physik. Chem.*, **160**, 45, 57 (1932). [i] Q_{6667} salts. [j] "International Critical Tables," McGraw-Hill Book Co., Inc., New York, N. Y., 1928. [k] F. A. Moelwyen-Hughes, "Physical Chemistry," Pergamon Press Ltd., London, 1961, p. 716. [l] A. Klemm in "Molten Salt Chemistry," M. Blander, Ed., Interscience Publishers, Inc., New York, N. Y., 1964, p. 564. [m] H. Reiss and S. W. Mayer, *J. Chem. Phys.*, **34**, 2001 (1961).

The first quantity, $\gamma/V^{1/3}$ (γ = surface tension in dyne cm.$^{-1}$, V = molar volume in cm.^{3}), was shown by Hildebrand and Scott[38] to be closely related to the internal pressure. We have made some preliminary measurements of the surface tension of three Q^+X^- at 153°: $Q_{5555}{}^+I^-$, 28; $Q_{5555}{}^+ClO_4^-$, 30; $Q_{5555}{}^+Pic^-$, 33 dyne-cm.$^{-1}$.[39] The corresponding $\gamma/V^{1/3}$ values are included in Table XIII.

Second, the energy of activation for viscous flow, ΔE_{vis}, was found by Ewell and Eyring[40] to be approx-

(34) I. M. Kolthoff, S. Bruckenstein, and M. K. Chantooni, Jr., *J. Am. Chem. Soc.*, **83**, 3927 (1961).
(35) C. A. Kraus, *J. Phys. Chem.*, **60**, 129 (1956).
(36) N. C. Deno and H. E. Berkheimer, *J. Org. Chem.*, **28**, 2143 (1963).
(37) J. H. Hildebrand, *J. Am. Chem. Soc.*, **38**, 1452 (1916).
(38) J. H. Hildebrand and R. L. Scott, "The Solubility of Nonelectrolytes," Reinhold Publishing Corp., New York, N. Y., 1950, p. 402.
(39) By capillary rise; melt densities interpolated from data of Walden and Birr, Table XIII, footnote *h*, for the corresponding isopentyl salts.
(40) Table XIII, ref. *d*.

imately proportional to the energy of vaporization. $\Delta E_{vis}/V$ should therefore afford another approximate measure of the cohesive energy density. The viscosity measurements of Walden and Birr[41] on three tetraisoalkylammonium salts afford values of this quantity given in Table XIII.

The final tabulated quantity is the transition energy of the charge-transfer band for 1-ethyl-4-carbomethoxypyridinium iodide, the empirical measure of solvent polarity (*Z*-value) studied by Kosower.[6] This excitation process corresponds to the (incomplete) annihi-

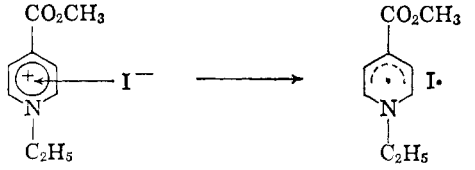

lation of charge in the ion pair, and is thus energetically related to the creation of a hole in a molten salt or dipolar nonelectrolyte medium.[36, 40, 42]

All three quantities agree closely in locating the molten Q^+X^- in the vicinity of acetone in Table XIII. This is a much lower rank on the polarity scale than might have been anticipated. Clearly these materials are far removed from the much more polar fused inorganic salts. This result, however, is in complete agreement with, and provides a clear physical basis for, the miscibility behavior of the Q^+X^- with liquid nonelectrolytes. Very widespread miscibility is observed with dipolar nonelectrolytes, which have cohesive energy densities similar to those of the Q^+X^-; miscibility becomes incomplete with liquids whose cohesive energy densities greatly exceed those of the Q^+X^-. The treatment of liquid–liquid solubilities given above is analogous to the discussion of solid Q^+X^- solubilities given by Deno and Berkheimer.[36] A final consequence of Table XIII is the prediction of low solubilities of inorganic salts in the molten Q^+X^-.

It is of interest to inquire whether the poorly cohesive character of the molten organic *vs.* the inorganic salts results solely from the decrease in interionic attraction with increasing ionic radius (illustrated by the sequence NaCl–CsI in Table XIII), or whether there is some further familial difference between the two fused salt categories. This question is most easily answered by computing γ for the Q^+X^- according to a theory of molten salt surface tension due to Reiss and Mayer[43] which gives good results for the inorganic salts. The pertinent expressions are

$$\gamma\ (\text{dyne cm.}^{-1}) = \frac{3kTy(y+2)}{2 \times 10^{-16}\pi a^2(1-y)^2};\quad y = \frac{\pi a^3 \rho N}{60M}$$

where a is the cation–anion distance of closest approach in Å., ρ is the density in g. cm.$^{-3}$, N is Avogadro's number, M is the molecular weight, k is the gas constant in erg deg.$^{-1}$, and T is the absolute temperature. Three independent estimates of a, the interionic distance of closest approach, can be made for, say, $Q_{5555}{}^+I^-$. Robinson's formula,[44] $r = 0.72V^{1/3}$, gives 5.29 Å. for the radius of $Q_{5555}{}^+$, and hence 7.5 Å. for a. The Stokes' law radius of $Q_{5555}{}^+$ is 5.25 Å.,[44] giving a = 7.4 Å. The Bjerrum distance of closest approach for tetraisopentylammonium iodide in benzene or ethylene chloride[35] is 5.9–6.2 Å. Taking a = 7.0 Å., one computes γ = 34 dyne cm.$^{-1}$ for $Q_{5555}{}^+I^-$ at 153° *vs.* 28 dyne cm.$^{-1}$ observed. This reasonably good agreement indicates that one probably need look no further than the ionic dimensions to account for the low position of Q^+X^- on the polarity scale.

Table XIII provides a chemical basis for the rule of thumb which one develops for the handling (with respect to solubility, nonhygroscopic nature, amenability to adsorption chromatography, *etc.*) of these QX– that they behave much as corresponding polar nonelectrolytes with X covalently attached as a functional group would be expected to do.

Solid State. The crystal chemistry of salts of the present type might be expected to be dominated by the large cation radii. $Q_{2222}{}^+I^-$ and $Q_{3333}{}^+Br^-$ are known to have four-coordinate, zinc sulfide type structures.[45, 46] Already in the case of $Q_{2222}{}^+I^-$ one unit cell dimension is fixed by cation–cation contacts,[45] and it is reasonable to suppose that, on enlarging Q to the tetrapentyl–tetraheptyl region, the anion has little influence on the structure. This would be consistent with the present finding of extensive isomorphism among Q^+X^- with X^- variable. For example, each of the Q^+I^-–$Q^+NO_3^-$ systems investigated (Q = Q_{5555}, Q_{6666}, Q_{6667}) showed continuous solid solubility although the difference in anion radius (2.16–1.75[47] = 0.41 Å., 23%) exceeds the usual *ca.* 15% limit.[48] Polymorphism, which appears to be widespread among these Q^+X^-, is also characteristic of the zinc blende–wurtzite type structures.[49]

We have confined the present work to salts containing no acidic or basic functional groups in the cation. However it is worth noting that the first organic salt chosen (by Stewart and Aston in 1926)[50] for a fused salt experiment, $C_2H_5OCH_2N(C_2H_5)_2CH_3{}^+I^-$, has a melting point (83°) considerably lower than the best attainable with saturated alkyl substituents.

(41) P. Walden and E. J. Birr, *Z. physik. Chem.*, 160, 45, 57 (1932).
(42) F. H. Stillinger, Jr., in "Molten Salt Chemistry," M. Blander, Ed., Interscience Publishers, Inc., New York, N. Y., 1964, p. 102 ff.
(43) H. Reiss and S. W. Mayer, *J. Chem. Phys.*, **34**, 2001 (1961).
(44) R. A. Robinson and R. H. Stokes, "Electrolyte Solutions," Academic Press Inc., New York, N. Y., 1959, pp. 124, 125.
(45) E. Wait and H. M. Powell, *J. Chem. Soc.*, 1872 (1958).
(46) A. Zalkin, *Acta. Cryst.*, 10, 557 (1957).
(47) L. Pauling, "The Nature of the Chemical Bond," Cornell University Press, Ithaca, N. Y., 1960, p. 547.
(48) R. C. Evans, "Crystal Chemistry," Cambridge University Press, London, 1964, p. 201.
(49) Reference 48, p. 144.
(50) T. D. Stewart and J. G. Aston, *J. Am. Chem. Soc.*, **48**, 1642 (1926).